Field induced metamagnetic transitions in quasi-one-dimensional Ising spin chain CoV_2O_6

M. Nandi and P. Mandal*
Saha Institute of Nuclear Physics, 1/AF Bidhannagar, Calcutta 700 064, India
(Dated: August 11, 2015)

We have investigated the temperature and magnetic field dependence of magnetization (M), specific heat (C_p), and relative sample length change ($\Delta L/L_0$) for understanding the field-induced metamagnetic transitions in quasi-one-dimensional monoclinic (α phase) and triclinic (γ phase) CoV_2O_6 spin chains. With the application of external magnetic field, a sharp peak emerges in $C_p(T)$ below T_N=15 K in α phase and a hump-like feature appears above T_N=6.5 K in γ phase due to the field-induced ferrimagnetic and ferromagnetic transitions, respectively. Strong field dependence of linear thermal expansion and large positive magnetostriction have been observed in α phase. Though magnetization data indicate strong spin-orbit coupling for both phases, other measurements show that this effect is very weak for the γ phase.
KEYWORDS: metamagnetic transition, Ising chain systems, spin-lattice coupling

I. INTRODUCTION

Cobalt based low-dimensional systems have drawn considerable attention in condensed matter physics due to their complex magnetic behavior. Such compounds having spin-chain structure exhibit strong magnetic anisotropy, field-induced metamagnetic transitions, 1/3 magnetization plateau, etc. For example, $Ca_3Co_2O_6$, which is constituted of Co^{3+} ion chains, exhibits cascade of magnetization plateaux.[1,2] Sometimes the plateau attains a value which is just 1/3 of the saturation magnetization such as in cobaltate dihydrate ($CoCl_2$:$2H_2O$).[3] Particularly, quasi one dimensional Ising spin chains display various fascinating magnetic phenomena like quantum criticality, order-disorder transition, etc. Ising spin chain $CoNb_2O_6$ is quite famous for the experimental evidence of quantum phase transition in transverse field.[4] For this system, an E_8 symmetry has been experimentally evidenced near the quantum critical point. Another well known Ising chain $BaCo_2V_2O_8$ exhibits peculiar order to disorder transition in presence of magnetic field.[5]

In recent years, quasi-one-dimensional Ising spin chain CoV_2O_6 has attracted immense interest because of the diverse magnetic transitions, large single ion anisotropy, strong spin-lattice coupling, etc. Depending on the local environment, CoV_2O_6 displays two different types of crystalline phases.[6–8] The high-temperature α phase crystallizes in a brannerite-like monoclinic structure,[6–14] while the low-temperature γ phase exhibits a triclinic structure.[6–8,15,16] In both the phases, the edge-sharing CoO_6 octahedra form magnetic chains along the b axis. These chains are separated by zigzag chains of VO_5 pyramids and VO_6 octahedra for the α and γ phase, respectively. The easy axis is perpendicular to chain direction in α phase[9,10] while it is pointing along the chain direction in γ phase.[17,18] The magnetic properties of CoV_2O_6 are solely determined by the divalent Co^{2+} ions because the V ions are in a nonmagnetic V^{5+} state. The Co^{2+} ions within the same chain are strongly coupled via ferromagnetic (FM) interaction while the interchain interaction is weak and antiferromagnetic (AFM) in nature. Both α and γ phases exhibit AFM to paramagnetic (PM) transition around 14 K and 6.5 K, respectively.[8,9,15]In this work, we present our results on magnetization, heat capacity and thermal expansion study for both α-CoV_2O_6 and γ-CoV_2O_6 compounds. Several important differences between field-induced magnetic states in these two systems are also discussed.

II. EXPERIMENTAL DETAILS

Polycrystalline α-CoV_2O_6 and γ-CoV_2O_6 samples were prepared by standard solid-state reaction method using the mixture of stoichiometric quantities of high purity V_2O_5 and cobalt acetate tetrahydrate or cobalt oxalate dihydrate. For α-CoV_2O_6, the mixture was heated in air for 16 h at 650°C and then at 725°C for 48 h. After the heat treatment, the material was quenched in liquid nitrogen to obtain single phase α-CoV_2O_6. For γ-CoV_2O_6, the mixture was heated in air at 620°C for 45 h and then cooled to room temperature at a rate of 2°C/min. The resulting powder was ground properly and pressed into pellets. Finally, the pellets were heated again at 620°C for 45 h and cooled at a rate of 2°C/min. Phase purity of these compounds was checked by powder x-ray diffraction (XRD) method with CuK_α radiation in a Rigaku TTRAX II diffractometer. No trace of impurity phase was detected within the resolution of XRD. All the peaks in

XRD were assigned to a monoclinic structure of space group $C2/m$ for α phase whereas to a triclinic structure of space group P-1 for γ phase using the Rietveld method. The magnetization measurements were done using a SQUID-VSM (Quantum Design). The specific heat measurements were done using a physical property measurement system (Quantum Design) by conventional relaxation time method. The thermal expansion measurements were done by capacitive method using a miniature tilted-plates dilatometer.

III. RESULTS AND DISCUSSION

The zero-field cool (ZFC) susceptibility (χ) and inverse susceptibility (χ^{-1}) versus temperature curves for both α and γ phases are presented in Figure 1. Measurements were performed at 0.1 T for both α phase and γ phase samples. For α phase, χ increases monotonically with decreasing temperature and exhibits a sharp peak around T_N=14 K due to the transition from PM to AFM state. Similar to α phase, $\chi(T)$ of γ phase also exhibits a sharp peak around 6.5 K due to the AFM transition. We observe that $\chi^{-1}(T)$ for both the compounds can be fitted well with the Curie-Weiss law [$\chi = N\mu_{eff}^2/3k(T-\theta)$] over a wide range of temperature as shown in Figure 1. From this Curie-Weiss fitting, we have calculated effective paramagnetic moment μ_{eff}=5.3 μ_B/Co ion and the Weiss temperature θ=-2.4 K for the α phase while the corresponding values are 5.2 μ_B/Co ion and -7 K for the γ phase. The negative θ indicates that the predominant magnetic interaction in these systems is antiferromagnetic in nature. The value of effective moment in paramagnetic state for both the compounds is much larger than the expected spin-only moment of high spin Co^{2+} (3.87 μ_B). We would like to mention that these values of μ_{eff} are comparable with those reported for polycrystalline and single crystalline samples.[12,15,18,19]

Isothermal magnetization curves at low temperature are plotted in Figure 2. The data were collected for field increasing condition at 5 K for the α phase and at 2 K for the γ phase. Even though these samples are magnetically random, particularly for α phase two sharp metamagnetic transitions are observed around two critical fields H_{c1} and H_{c2}. α-CoV_2O_6 exhibits field-induced transitions from AFM to ferrimagnetic (FI) state at H_{c1} ($\sim$ 1.5 T) followed by FI to FM state at H_{c2} ($\sim$ 3.3 T) with a 1/3 magnetization plateau when the magnetic field is applied parallel to the c axis. Similar to α-CoV_2O_6, γ-CoV_2O_6 also exhibits two successive metamagnetic transitions with 1/3 magnetization plateau along easy axis. However, the anomalies around two critical fields for the γ-CoV_2O_6 are not clearly visible in $M(H)$ curve even at 2 K. To track the critical fields, we have calculated the derivative of $M(H)$ which exhibits two peaks around two critical fields. The critical fields H_{c1} and H_{c2} determined in this way are about 0.4 T and 0.6 T, respectively. These values are close to earlier reports.[8,15] Two field-induced transitions are clearly observed even for the magnetically random α-phase sample while these two transitions are not clearly separated in the $M(H)$ curve of magnetically random γ-phase sample. Actually, the values of critical fields as well as the difference between two critical fields for the γ phase are very small as compared to that for the α phase. For this reason, the anomalies around two critical fields are not distinguishable in magnetically random γ-phase sample. Though the chemical formula is same for both phases, the structures are quite different. The strength of magnetic interaction is mainly determined by the interatomic distances. In γ-phase, the interchain distance is larger compared to α phase.[8] Due to the larger interachain distance, the antiferromagnetic interaction is weaker in γ-phase as compared to α-phase which is reflected in their ground state ordering temperature. The antiferromagnetic ordering temperature for the γ-phase is just half of that for the α-phase. As the interchain coupling is much weaker in γ-phase, a smaller field is required to align the chains ferromagnetically. For this reason, γ-phase has smaller critical fields as compared to that for the α-phase.

Specific heat (C_p) versus temperature curves in the vicinity of T_N are shown in Figures 3 (a) and (b) for some selected magnetic fields for α-CoV_2O_6 and γ-CoV_2O_6, respectively. At zero field, a λ-like peak has been observed around T_N. For the α phase, when the external magnetic field is applied, the peak at T_N gradually suppresses, broadens and shifts towards lower temperature. Apart from this, an interesting behavior with application of magnetic field is observed. For example, a new peak appears around 11 K for applied field of 2.5 T due to the field-induced FI transition. This field-induced peak remains clearly visible even at field as high as 8 T. To determine the exact positions of the peaks, we have deconvoluted the peaks. A pair of Gaussian functions plus a suitable background was fitted to the data. It is observed that the peak positions shift slowly with field. Also, the field-induced peak is found to be quite sharp, possibly due to the first-order nature of the transition. Unlike α-CoV_2O_6, a clear hump-like feature appears well above T_N in C_p data of γ-CoV_2O_6 due to the emergence of a FM phase when the applied magnetic field exceeds a critical value. For example, this hump-like feature occurs around 9.5 K ($\sim T_F$) at 2 T and shifts slowly towards higher temperature with increase of magnetic field. Closer inspection reveals that another very weak anomaly appears around 5 K ($\sim T_{FI}$) due to the FI phase. Though both these two features are observable at 1 T, they are more clearly

visible at 2 T and above [inset of Figure 3(b)]. With the increase of magnetic field strength, the hump-like feature pronounces whereas the peak at T_N and the weak anomaly just below T_N progressively suppress. At 5 T and above, only the hump-like feature survives. In a magnetically random sample, different ordered magnetic phases coexist. When the applied field is greater than H_{c1} (H_{c2}), the system contains a certain fraction of FI (FI and FM) phase. The reported low-temperature neutron diffraction results also support this observation.[10] For α phase, powder neutron diffraction studies have revealed that both AFM and FI phases coexist with percentage of 54 and 46, respectively at 2.5 T. At fields above H_{c2}, however, AFM, FI and FM phases coexist and with further increase of field strength AFM and FI fractions decrease significantly due to the increase of FM phase.

In order to investigate the spin-orbit coupling and field-induced transitions in more details, we have also studied the linear expansion of sample length [$\Delta L/L$] as functions of T and H. For α-CoV_2O_6, the temperature dependence of $\Delta L(T)/L_{4K}$ (=[$L(T)$-L_{4K}]/L_{4K}) up to 35 K for some selected fields has been plotted in Figure 4 (a), where L_{4K} is the length of the sample at T=4 K in an applied field H. At zero field, $\Delta L/L_{4K}$ shows a sharp anomaly around T_N. At 2.5 T, $\Delta L(T)/L_{4K}$ exhibits a step-like decrease below the antiferromagnetic transition temperature. For understanding the field-induced anomalies at and below T_N, we have calculated thermal expansion coefficient (α) at different fields. The temperature dependence of α is shown in Figure 4(b). It is clear from the figure that $\alpha(T)$ curves are qualitatively similar to that of $C_p(T)$ curves. At zero field, $\alpha(T)$ exhibits a λ-like peak around T_N. With the application of magnetic field, a very sharp peak appears below T_N which remains visible up to 4 T. Thus, similar to specific heat data, the field-induced transitions are reflected in thermal expansion measurements. For the polycrystalline sample, though the linear thermal expansion gives an average expansion along three crystallographic axis directions, the field-induced features in thermal expansion is observed mainly due to the change of c axis length. Our results on thermal expansion is consistent with reported data of temperature variation of lattice parameters determined using powder neutron diffraction[12,13].

Figure 5 presents a comparison between the magnetostriction, $\Delta L(H)/L_0$=[$L(H)$-L_0]/L_0, where L_0 is the length of the sample in absence of magnetic field, and magnetization for α-CoV_2O_6. It is clear from Figure 5 that the magnetostriction is very sensitive to temperature and displays a huge value at low temperature. At 3 K, $\Delta L/L_0$ exhibits two sharp anomalies around two critical fields of metamagnetic transitions. Magnetostriction curve also shows strong hysteresis similar to that observed in magnetization data at 3 K. Above T_N, these two anomalies disappear in magnetostriction as well as in magnetization curve. We have also measured magnetostriction at temperatures well above T_N and observed no anomaly. For example, $\Delta L/L_0$ at 35 K increases monotonically with temperature like magnetization curve (inset of Figure 5). It is clear from Figure 5 that $\Delta L(H)/L_0$ is large and approximately mimics the nature of $M(H)$ curve for α phase. So it can be concluded that there exists a strong spin-lattice coupling in α phase. We would like to mention that the linear expansion of sample length as functions of both T and H have also been measured for γ phase. In contrast to α phase, a very weak anomaly has been observed in $\Delta L/L_{4K}$ versus T curve around T_N and no other field-induced transition has been found. The value of magnetostriction is also very small as compared to α phase.

IV. CONCLUSIONS

In conclusion, we have compared and contrasted different physical properties of quasi-one-dimensional antiferromagnetic monoclinic and triclinic spin chains of CoV_2O_6. For both the phases, $C_p(T)$ exhibits a sharp λ-like peak around T_N. Though C_p of both phases exhibit strong T and H dependence, appeared features in $C_p(T)$ due to the external magnetic field are different for two phases. When the applied field exceeds a certain critical field, a sharp peak appears below T_N due to the ferrimagnetic-paramagnetic transition for α phase whereas a weak anomaly below T_N and a hump-like feature above T_N appear in γ phase due to FI-PM and FM-PM transitions respectively. Similar to $C_p(T)$, thermal expansion coefficient also exhibits emergence of field-induced peak below T_N in α-CoV_2O_6. Huge magnetostriction effect has been found below T_N in α phase. So, it indicates that the spin-lattice coupling in α phase is quite strong. For γ phase, linear expansion $\Delta L/L_{4K}$ exhibits a very weak anomaly around T_N and no significant amount of magnetostriction has been observed. So it can be concluded that the spin-lattice coupling is very weak in γ phase compared to α phase.

* Electronic address: prabhat.mandal@saha.ac.in

[1] A. Maignan, V. Hardy, S. Hebert, M. Drillon, M. R. Lees, O. Petrenko, D. M. K. Paul, and D. Khomskii, J. Mater. Chem. 14 (2004) 1231.
[2] A. Maignan, C. Michel, A. C. Masset, C. Martin, and B. Raveau, Eur. Phys. J. B 15 (2000) 657.
[3] H. Kobayashi and T. Haseda, J. Phys. Soc. Jpn. 19 (1964) 765.
[4] R. Coldea, D. A. Tennant, E. M. Wheeler, E. Wawrzynska, D. Prabhakaran, M. Telling, K. Habicht, P. Smeibidl, and K. Kiefer, Science 327 (2010) 177.
[5] Z. He, T. Taniyama, K$\hat{y}$omen, and M. Itoh, Phys. Rev. B 72 (2005) 172403.
[6] N. Hollmann, S. Agrestini, Z. Hu, Z. He, M. Schmidt, C.-Y. Kuo, M. Rotter, A. A. Nugroho, V. Sessi, A. Tanaka, N. B. Brookes, and L. H. Tjeng, Phys. Rev. B 89 (2014) 201101(R).
[7] B. Kim, B. H. Kim, K. Kim, H. C. Choi, S. Y. Park, Y. H. Jeong, and B. I. Min, Phys. Rev. B 85 (2012) 220407(R).
[8] M. Lenertz, J. Alaria, D. Stoeffler, S. Colis, and A. Dinia, J. Phys. Chem. C 115 (2011) 17190.
[9] Z. He, J. Yamaura, Y. Ueda, and W. Cheng, J. Am. Chem. Soc. 131 (2009) 7554.
[10] M. Lenertz, J. Alaria, D. Stoeffler, S. Colis, and A. Dinia, Phys. Rev. B 86 (2012) 214428.
[11] K. Singh, A. Maignan, D. Pelloquin, O. Perez, and Ch. Simon, J. Mater. Chem. 22 (2012) 6436.
[12] M. Markkula, A. M. Arevalo-Lopez, and J. P. Attfield, J. Solid State Chem. 192 (2012) 390.
[13] M. Markkula, A. M. Arevalo-Lopez, and J. P. Attfield, Phys. Rev. B 86 (2012) 134401.
[14] M. Nandi, N. Khan, D. Bhoi, A. Midya and P. Mandal, J. Phys. Chem. C 118 (2014) 1668.
[15] S. A. J. Kimber, H. Mutka, T. Chatterji, T. Hofmann, P. F. Henry, H. N. Bordallo, D. N. Argyriou, and J. P. Attfield, Phys. Rev. B 84 (2011) 104425.
[16] Z. He and M. Itoh, J. Crystal Growth 388 (2014) 103.
[17] M. Lenertz, S. Colis, C. Ulhaq-Bouillet and A. Dinia, Appl. Phys. Lett. 102 (2013) 212407.
[18] M. Lenertz, A. Dinia, and S. Colis, J. Phys. Chem. C 118 (2014) 13981.
[19] Y. Drees, S. Agrestini, O. Zaharko, and A. C. Komarek, Cryst. Growth Des. **15**, 1168 (2015).

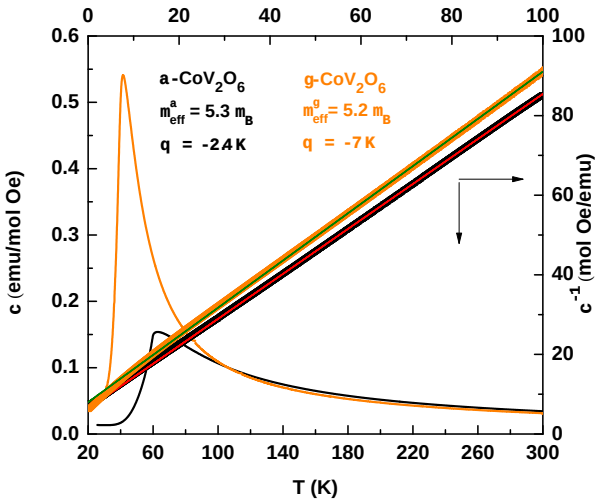

Fig.1 (Nandi et al.)

FIG. 1: Temperature dependence zero-field-cool susceptibility (χ) for α-CoV_2O_6 and γ-CoV_2O_6 at 0.1 T. The right axis shows the inverse of susceptibility (χ^{-1}) and the corresponding Curie-Weiss fit (solid line).

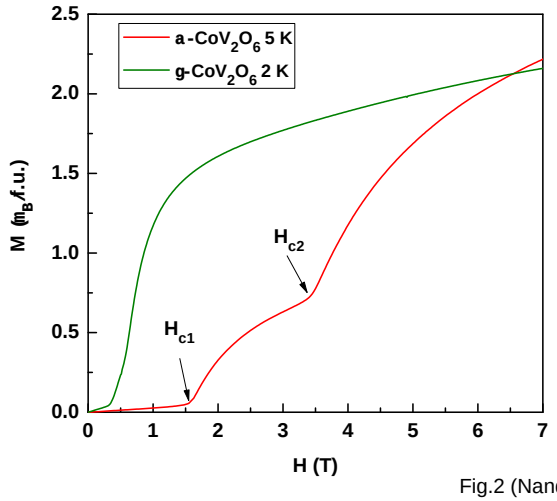

Fig.2 (Nandi et al.)

FIG. 2: Isothermal magnetization for α-CoV_2O_6 and γ-CoV_2O_6 at 5 K and 2 K respectively.

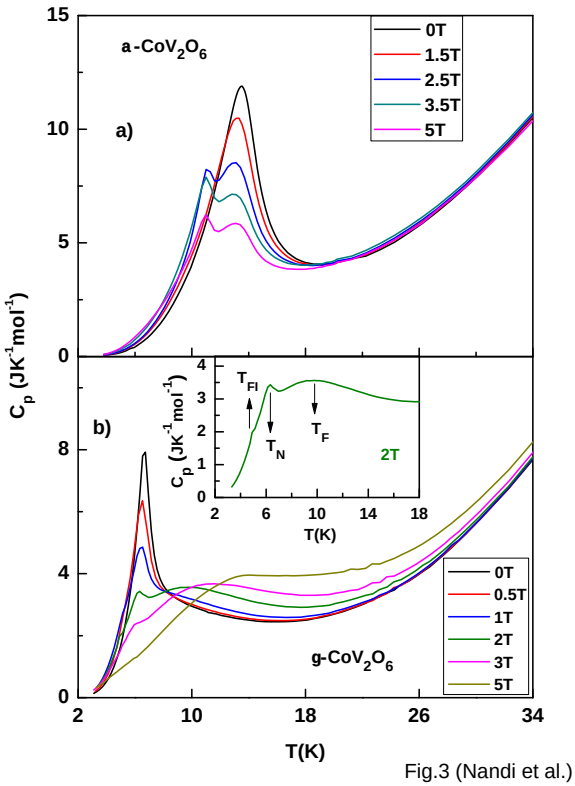

FIG. 3: (a) and (b) Temperature dependence of specific heat of α-CoV_2O_6 and γ-CoV_2O_6, are plotted for selected fields, respectively. Inset: Zoomed view of $C_p(T)$ at 2 T of γ-CoV_2O_6, indicating three anomalies around three transition temperatures T_N, T_{FI} and T_F.

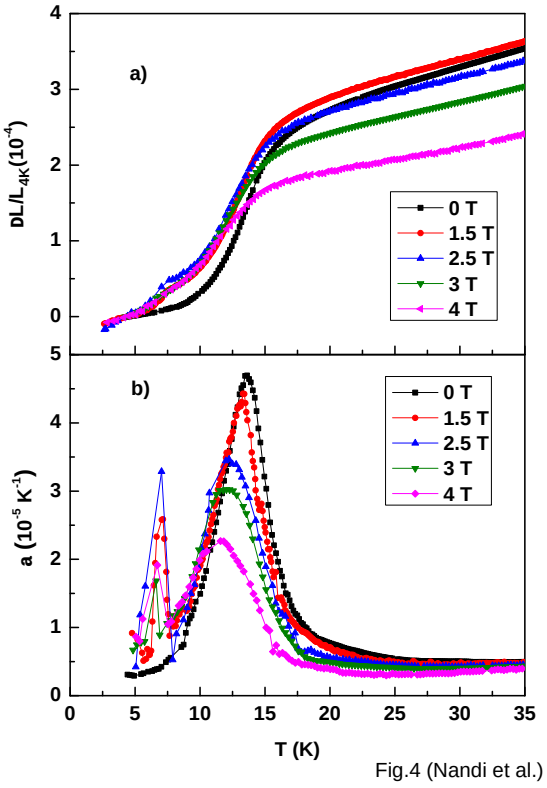

FIG. 4: (a) The temperature dependence of the relative length change ($\Delta L/L_{4K}$) for α-CoV_2O_6 for different fields. (b) Plots of the thermal expansion coefficient $\alpha(T)$ for different fields.

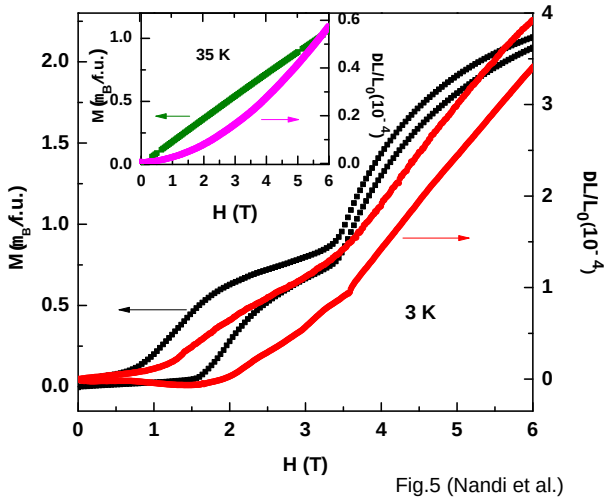

FIG. 5: Magnetostriction, $\Delta L(H)/L_0$, and magnetization for both increasing and decreasing field at 3 K for α-CoV_2O_6. Inset: the field dependence of magnetization and $\Delta L/L_0$ at 35 K.